Publishing Excellence
Inspiring Progress
ARISTON PUBLICATIONS
SciEngg Advances
ISSN: 0000-0000 www.aristonpubs.com/sciengg-advances https://doi.org/10.69626/csa.2024.0020

RESEARCH ARTICLE

Design and Evaluation of a Twin-Core Photonic Crystal Fiber Sensor for Human Blood Biomolecules

Vikash Mourya[1], Sapana Yadav[1], D.K. Dwivedi[1], Pooja Lohia[2]

ABSTRACT: A twin-core photonic crystal fiber (TC-PCF) sensor is proposed featuring a rectangular analyte channel, designed for blood component detection. The cladding area of this sensor incorporates rectangular air-holes, with silica serving as the substrate material. Operating within a wavelength range of 2 µm to 3 µm. The sensor's modeling and simulation is conducted by using COMSOL Multiphysics software, while schematic curves were plotted using Origin software. This TC-PCF sensor demonstrates remarkable sensitivity, reaching 1641.2 nm/RIU for white blood cells and 2732.638 nm/RIU for red blood cells. Offering a compact and advanced solution, this sensor addresses challenges commonly encountered with traditional blood biomolecule sensors. Its cost-effectiveness and ease of fabrication may lead the proposed sensor structure for promising future applications.

Keywords: Twin-core photonic crystal fiber, Transmission, Wavelength sensitivity, Blood component.

Received: 03 January 2024; Revised: 15 February 2024; Accepted: 05 March 2024; Available Online: 21 March 2024

1. INTRODUCTION

In 1996, optical fibers (OFs) were developed for sensing and telecommunications. This breakthrough paved the way for the advancement of precise and sensitive systems guided by light [1]. Knight et al. were the pioneers in reporting about photonic crystal fibers (PCFs) [2]. Due to ongoing scientific progress, PCFs have garnered significant attention due to their exceptional sensitivity, stability, compact size, flexible design, and multiplexing capabilities [3]. These PCF sensors demonstrate effectiveness even in challenging conditions such as noise, intense electromagnetic waves, extreme temperatures, and high voltage [4]. They find broad applications across various fields, serving purposes like biosensors [5–8] , remote sensing [9], spectroscopy [10], chemical sensing [11–14], laser applications [15], pressure sensing [16, 17], temperature sensing [18], and more. Silica serves as the foundational material in this twin core photonic crystal fiber (TC-PCF) sensor due to its low optical losses within specific wavelength ranges and its wide, transparent optical window, enabling light transmission across a broad spectrum of wavelengths. Now a days photonic crystal fiber-based sensors are used for sensing the biological components. The sensor used for sensing biological components are known as bio-sensors. Red blood cells, platelets, white blood cells, water and plasma constitute the essential components of blood, a highly specialized tissue composed of approximately 4000 distinct elements [19]. Each year, a significant number of fatal infections directly linked to human blood leads to 36 million deaths. In a healthy individual, blood accounts for 7% of the body's weight [20, 21]. It is widely recognized that blood consists of solid components like white blood cells (WBCs), red blood cells (RBCs), alongside liquid plasma, which is primarily 90% water. In the typical human body, RBCs comprise about 4% of the volume, plasma about 54%, WBCs about 0.7%, and

[1] Photonics and Photovoltaic Research Lab (PPRL), Department of Physics and Material Science, Madan Mohan Malaviya University of Technology, Gorakhpur-273010, India

[2] Department of Electronics and Communication Engineering, Madan Mohan Malaviya University of Technology, Gorakhpur-273010, India.

* Author to whom correspondence should be addressed: todkdwivedi@gmail.com (D. K. Dwivedi)

the remaining 10% consists of proteins, nutrients, and ions [21].

Presently, there exist numerous sensor configurations based on PCF for diverse applications, with ongoing analysis aimed at the most optimized parameters. Islam et al. suggested the PCF sensor with square air-holes & core with topas as a background material and the attained sensitivity rates for RBCs, hemoglobin, WBCs, plasma, and water for y-polarization are 99.39%, 99.27%, 99.12%, 99.03%, and 98.79%, respectively [22]. Hossain et al. proposed a sensor with rectangular air-holes as well as the rectangular core too. The achieved relative sensitivities are 89.14% for water, 90.48% for plasma, 91.25% for white blood cells (WBCs), 92.41% for hemoglobin and 93.50% for red blood cells (RBCs) [8]. Eid et al. proposed a sensor which demonstrates exceptionally high Relative Sensitivity percentages of 95.80% for RBCs, 95% for hemoglobin, 93.60% for WBCs, 92.50% for plasma, and 91.40% for water [23].

In this study, a biosensor utilizing a simple twin-core photonic crystal fiber (TC-PCF) is developed for detecting blood components, featuring square air-holes and analyte channel. Computational analysis is carried out using COMSOL Multiphysics software with the finite element method (FEM). The blood sample is introduced into the analyte channel. The investigation reveals that the TC-PCF sensor achieves the highest wavelength sensitivity of 2732.638 nm/RIU over a fiber length of 300 µm.

2. SENSOR DESIGN AND PERFORMANCE PARAMETERS

The suggested T-PCF sensor's cross-sectional image features an arrangement of rectangular air-holes forming a rhombical shape and two cores distinguished by a central rectangular air-hole, as depicted in Figure 1. Silica glass is served as the background material for the proposed TC-PCF. The inner rectangular air-holes are defined by R_1 and outer rectangular air-holes by R_2 with the center-to-center distance between air-holes known as pitch (Λ) and the central air-hole or the analyte channel is defined by R_3. The analyte is to be introduced into the central air-holes since it is referred to as the 'analyte channel'. This channel is positioned between the cores of the recommended sensor to ensure proper interaction between the analyte and the electric field as light propagates through the fiber. The design and simulation of the TC-PCF is conducted using COMSOL Multiphysics software. The computational meshing domain comprises a total no. of 1418 elements, with 338 boundary elements and 44 vertex elements, as illustrated in Figure 2. Figure 3 depicts the experimental setup for the proposed TC-PCF.

Table 1. Refractive index of blood components.

Blood Component	Refractive Index (RI)	References
Water	1.33	
WBCs	1.36	[24]
RBCs	1.40	

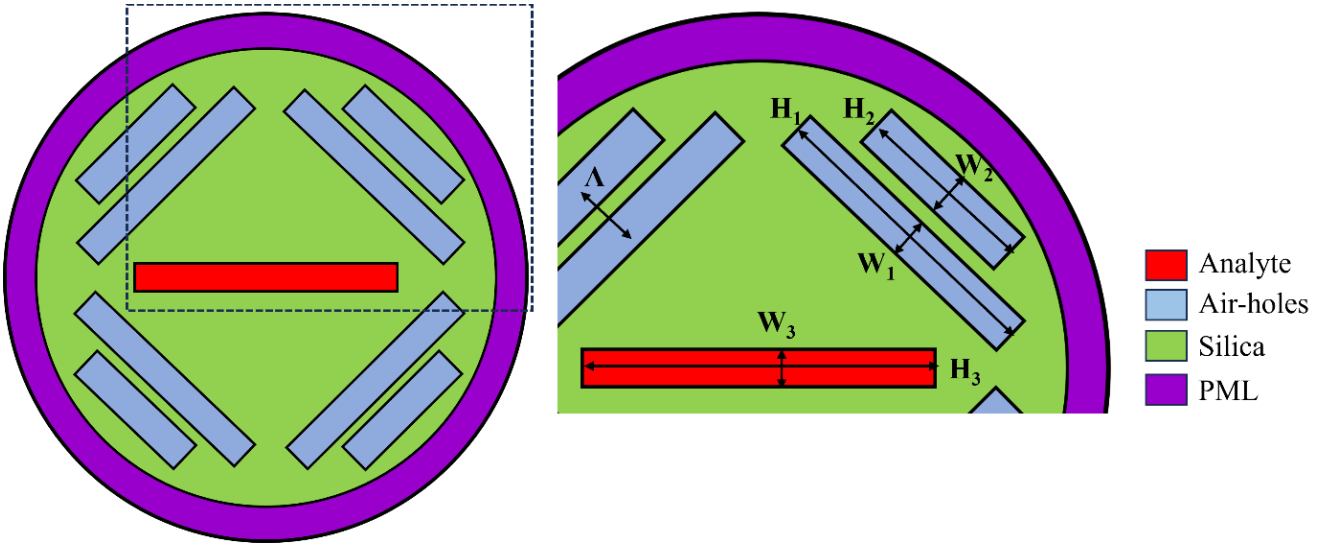

Fig. 1. Cross-sectional view of TC-PCF

To enhance endurance, power, and protection against external factors, a perfectly matched layer (PML) is incorporated into the fiber. The refractive index (RI) of the surrounding medium significantly influences propagation through the core region. The RI of blood components is given in Table-1.

The outer rectangular air-holes (R_1) are arranged in a clockwise rotation of 90 degrees, with a width of 0.75 µm (W_2) and height of 3.25 µm (H_2). Similarly, the inner rectangular air-holes (R_2) are arranged in a clockwise rotation of 90 degrees, with width of 0.75 µm (W_1) and height of 5.25 µm (H_1). The pitch (Λ) between the outer and inner loop air-holes is 2 µm. The central rectangular air-hole (R_3) with the width of 0.75 µm (W_3) and height of 6.25 µm (H_3). The fiber diameter, excluding the perfectly matched layer (PML) is 11 µm. Furthermore, a PML layer with a thickness of 0.75 µm has been introduced.

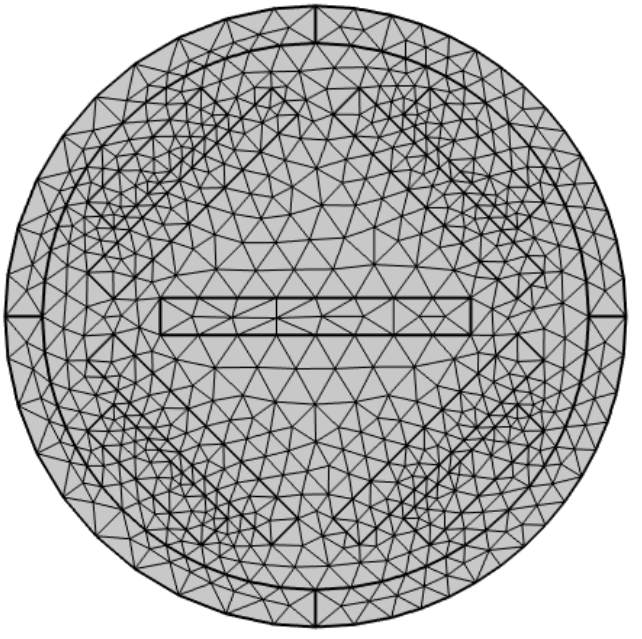

Fig. 2. Computational grid for suggested TC-PCF.

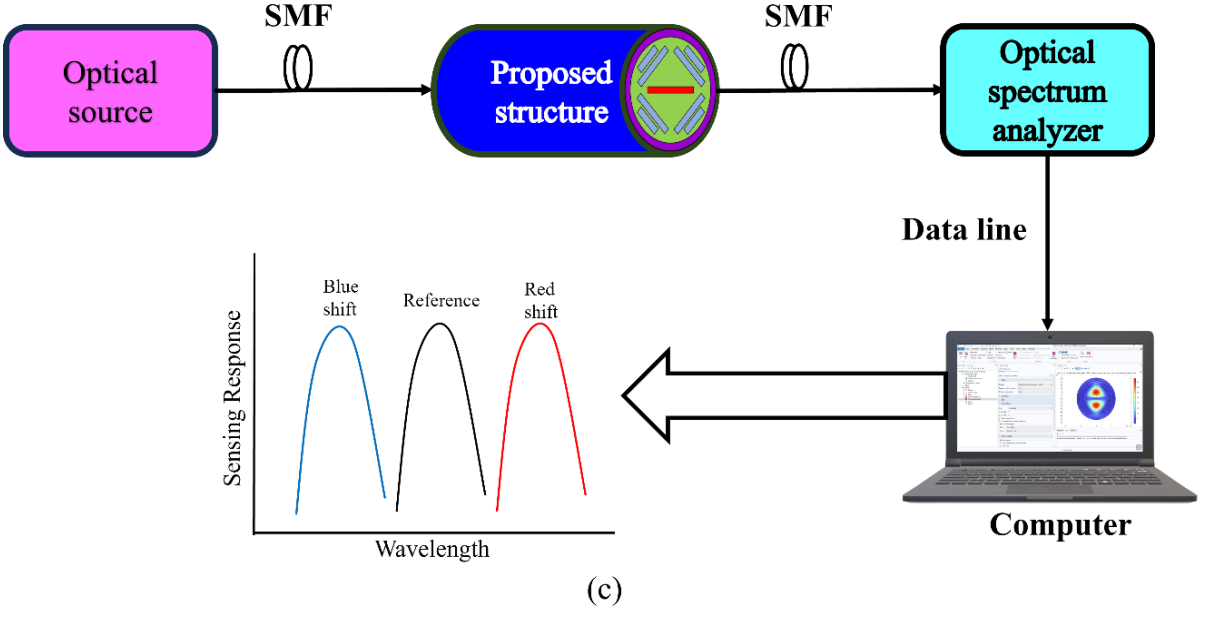

Fig. 3. Generalized experimental setup for proposed TC-PCF.

The RI of silica is evaluated by the Sellmeier equation as given below [25, 26]:

$$n(\lambda)^2 \text{ silica} = a + \frac{0.696\lambda^2}{\lambda^2 - 0.00047} + \frac{0.408\lambda^2}{\lambda^2 - 0.14} + \frac{0.897\lambda^2}{\lambda^2 - 97.934} \quad (1)$$

In the present TC-PCF, the electric field distribution resulting from the sensor's dual cores generates four super modes in both x and y polarizations. These super modes are classified as x_{even}, x_{odd}, y_{even}, and y_{odd}. Figure 4 illustrates the electric field distribution for the suggested TC-PCF and Figure 5 represents electric field intensity (3D perspective) for x_{even}, x_{odd}, y_{even}, and y_{odd}.

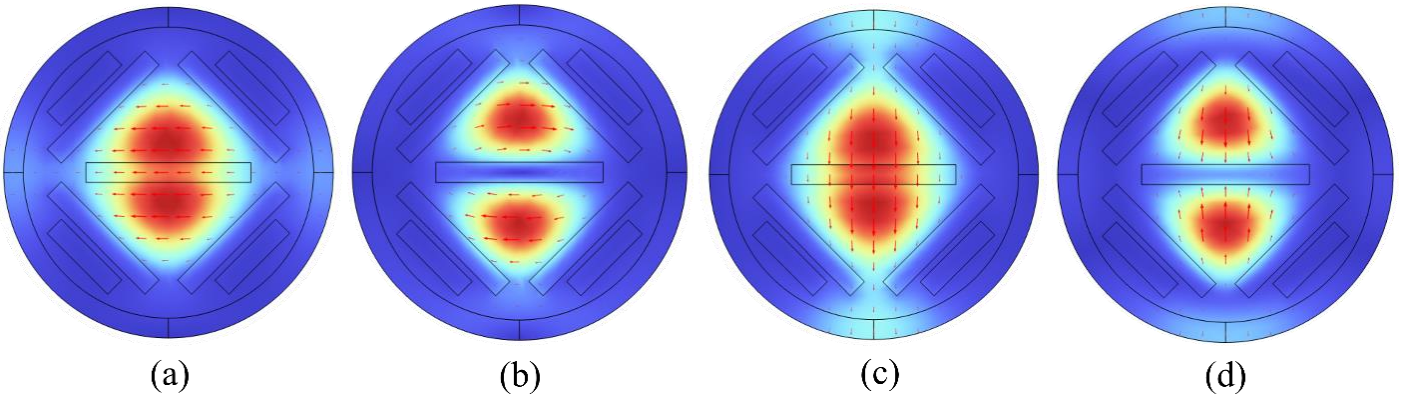

Fig. 4. Distribution of electric field for the four super-modes (a) x_{even} (b) x_{odd} (c) y_{even} (d) y_{odd}.

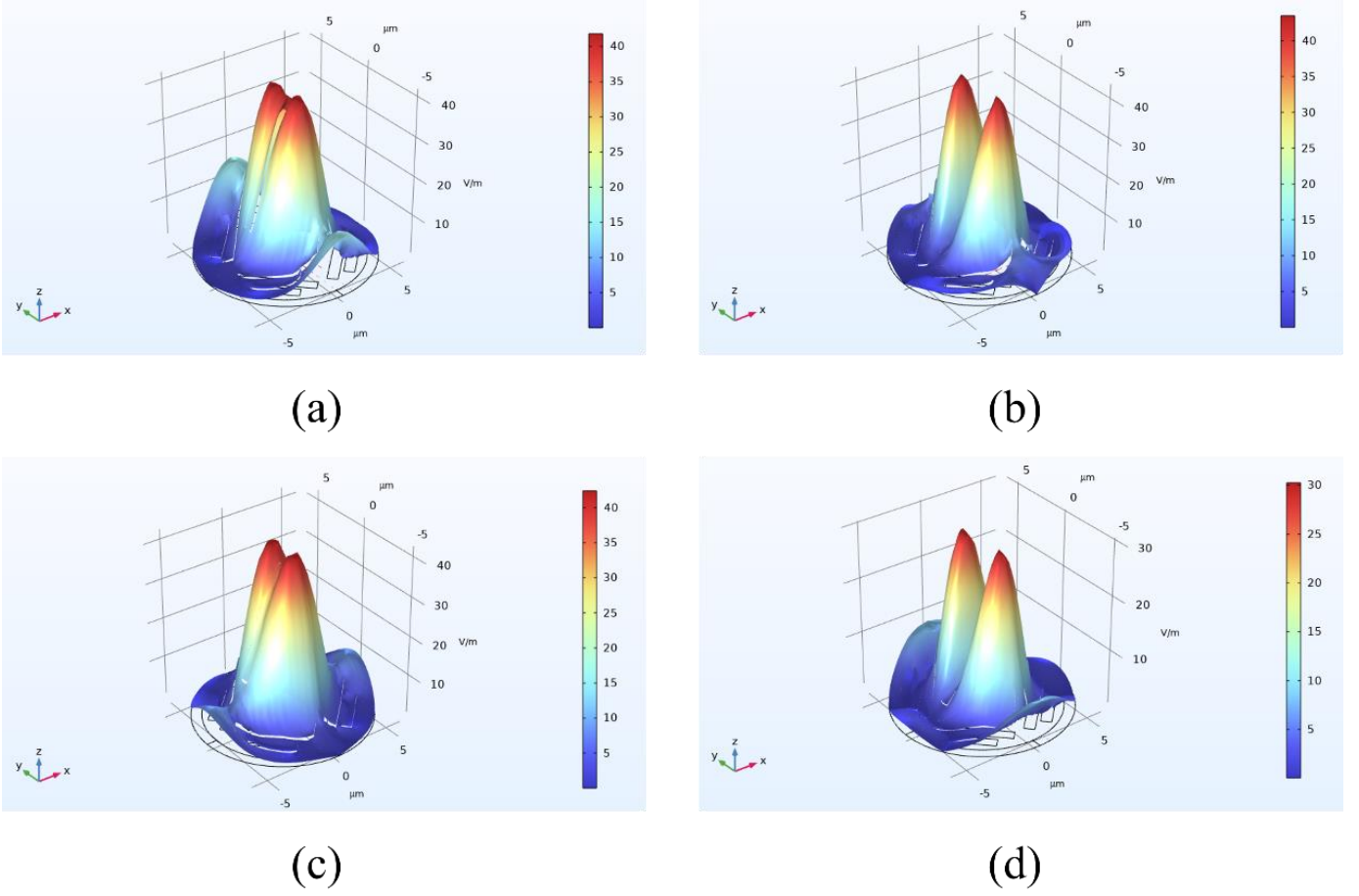

Fig. 5. Electric field intensity (3D perspective) for (a) x_{even} (b) x_{odd} (c) y_{even} (d) y_{odd}.

2.1. Birefringence

Birefringence refers to the variation in the real component of the effective refractive index among different modes of x-polarization and y-polarization. This can be calculated using a specific equation [27]:

$$Bi = |n^i_{even} - n^i_{odd}| \qquad \text{where, } i = x, y \tag{2}$$

2.2. Coupling Length

Once the birefringence value is obtained, another vital parameter used to assess the performance of PCF or the distance over which power transmission takes place is known as the coupling length (L_C) [28]. It is given by:

$$L_c = \frac{\pi}{|\beta^i_{even} - \beta^i_{odd}|} = \frac{\lambda}{2|n^i_{even} - n^i_{odd}|} = \frac{\lambda}{2B^i} \ (\mu m) \tag{3}$$

2.3. Power Shift

The theory of mode coupling suggests that the optical power transmitted from one core to another across the length of the fiber can be evaluated in the following manner [29]:

$$I_i(\lambda) = \sin^2\left(\frac{\pi \triangle n^i L}{\lambda}\right) \qquad \text{with, } i = x, y \tag{4}$$

Where, $\triangle n^i = |n^i_{even} - n^i_{odd}|$. Maximum value of the transmission curve is at unity and it is sinusoidal in nature.
In the proposed DC-PCF, optical power includes both the x & y polarization. Since these polarizations are mutually perpendicular, the overall output can be characterized by [29]:

$$I(\lambda) = I_x + I_y \tag{5}$$

By combining equation (4), and (5), the total intensity of the output can be calculated by [29]:

$$I(\lambda) = 1 - \cos\left[\frac{\pi(\triangle n^i_x + \triangle n^i_y)L}{\lambda}\right].\cos\left[\frac{\pi(\triangle n^i_x - \triangle n^i_y)L}{\lambda}\right] \tag{6}$$

2.6. Confinement Loss

Confinement loss, an essential parameter indicating light leakage, arises from the waveguide structure and is evident in single-material fibers like Photonic Crystal Fiber (PCF). The formula representing this phenomenon is as follows [30]:

$$\text{Confinement loss} = \frac{40\pi}{\ln(10)\lambda} \times \text{Img}(n_{eff}) \times 10^4 \ (\text{dB/cm}) \tag{7}$$

Here, Img(n_{eff}) is the imaginary effective refractive index.

2.5. Wavelength Sensitivity

Wavelength sensitivity for the suggested DC-PCF can be calculated by evaluating the wavelength shift in the transmission spectrum. The wavelength sensitivity is given by [31]:

$$S_\lambda = \frac{\triangle \lambda_{peak}}{\triangle n^i} \ (\text{nm/RIU}) \tag{8}$$

Where, $\triangle\lambda_{peak}$ is maximum peak to peak wavelength and it can be calculated by $\triangle\lambda_{peak} = \triangle\lambda_{blood\ component} - \triangle\lambda_{water}$; $\triangle n^i$ is the difference in refractive index and it can be evaluated by $\triangle n^i = \triangle n^{blood\ component} - \triangle n^{water}$ [32].

3. 3. RESULT AND DISCUSSION

In the proposed study, a numerical evaluation of photonic crystal fiber (PCF) has been carried out, examining different samples including water, WBCs & RBCs. The analysis employed the finite element method to investigate parameters such as effective refractive index, birefringence, coupling length, power shift, wavelength sensitivity and confinement loss across various guiding wavelengths ranging from 2 µm to 3 µm. The accompanying graphs, derived from the study, are provided for reference. Figure 6. represents the graphs for the effective refractive index (ERI). From the Figure 6 it is observed that ERI decreases with the increase in wavelength.

Figure 7 illustrates the birefringence curve for both x and y-polarization within the wavelength range of 2 µm to 3 µm across different blood component samples suggested for the TC-PCF sensor. Figure 7 indicates a trend where birefringence rises alongside wavelength increments. The highest birefringence is at the wavelength of 3 µm. The highest birefringence values for x-polarization are 0.029, 0.323 & 0.378 for water, WBC, RBC respectively and for y-polarization the values are 0.0328, 0.359 and 0.414 for water, WBC and RBC, respectively.
Observing equation (2) and (3), it is noted that the coupling length and birefringence exhibit inverse proportionality. Figure 8 illustrates the coupling length curve with wavelength for both x-polarization and y-polarization. It is evident from the graphs that as the wavelength increases, the coupling length decreases.The highest coupling length values for x-polarization are 103.09 µm, 96.15 µm and 69.44 µm for water, WBC and RBC, respectively and the highest value for y-polarization are 94.34 µm, 90.09 µm, and 67.57 µm for water, WBC, and RBC, respectively.

The confinement loss for the suggested TC-PCF is 4×10^{-6} dB/cm at 2.9 µm for water, 7.09×10^{-6} dB/cm at 2.4 µm for WBC and 1.56×10^{-6} dB/cm at 2 µm for RBC as shown in Figure 9.

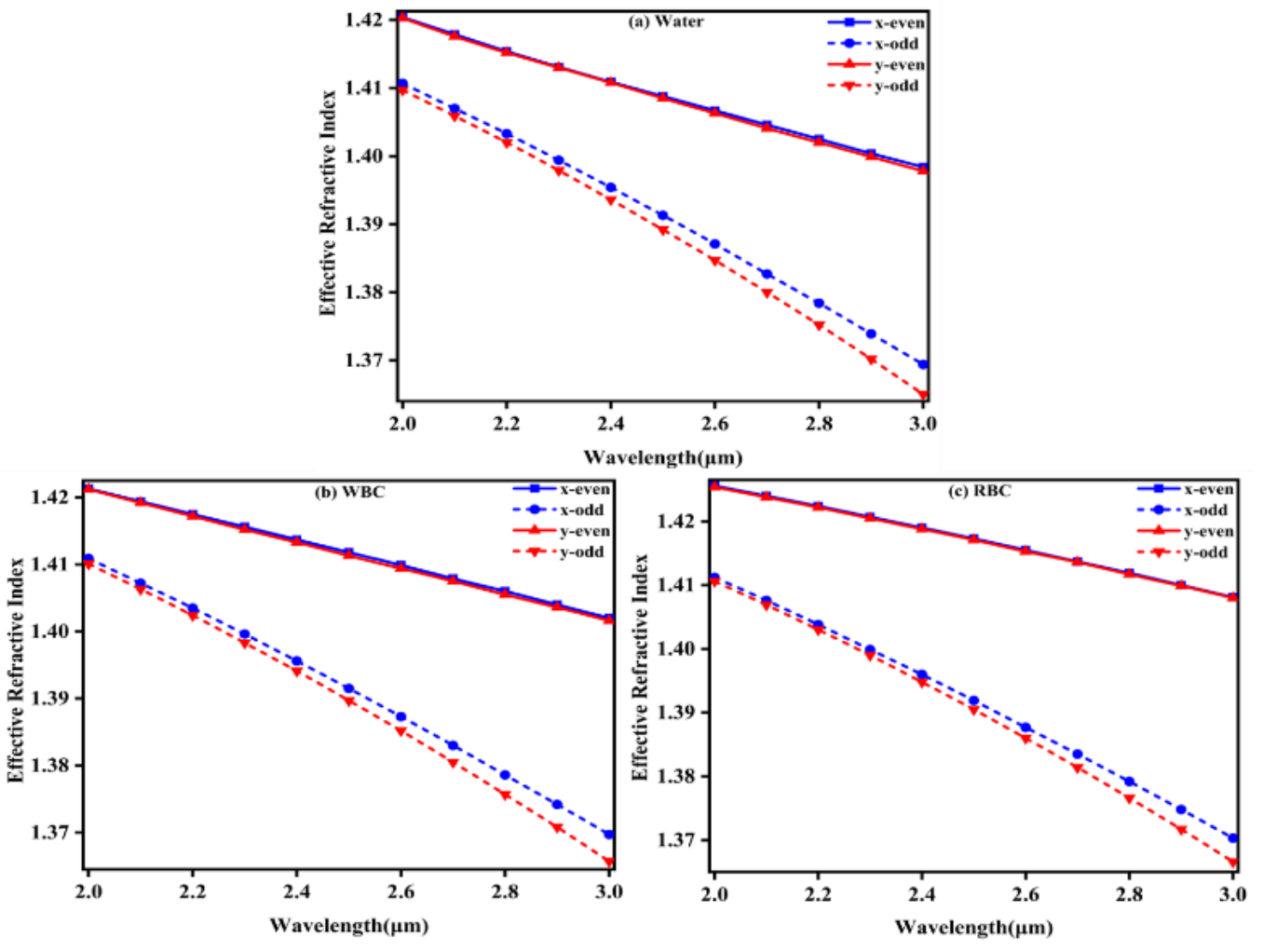

Fig. 6. Variation of Effective refractive index with Wavelength for structure-1 for (a) Water (b) WBC (c) RBC.

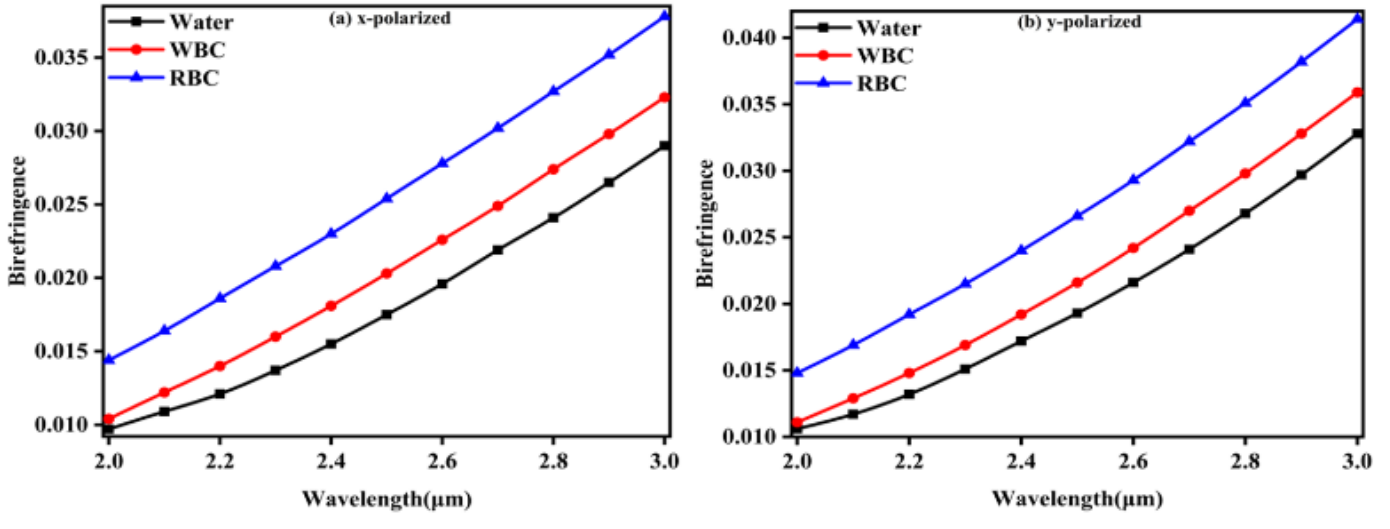

Fig. 7. Birefringence curve with wavelength for (a) x-polarized (b) y-polarized.

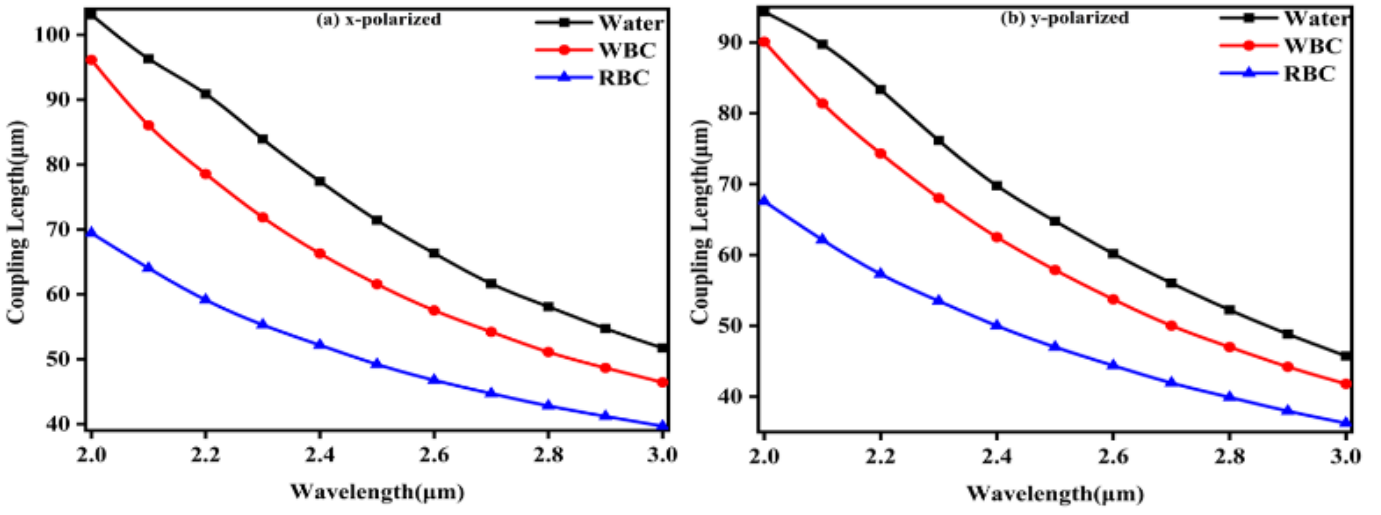

Fig. 8. Coupling length curve with wavelength for (a) x-polarized (b) y-polarized.

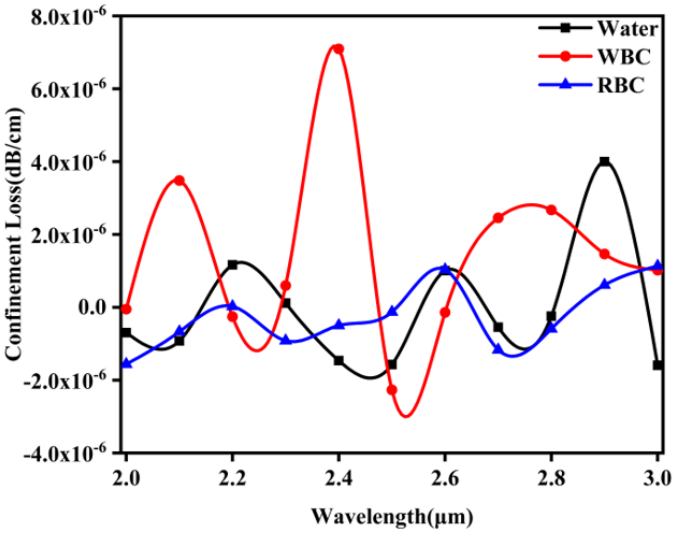

Fig. 9. Variation of Confinement loss with Wavelength.

The transmission spectrum for the various blood components analyte is shown in Fig. 10 for the fiber length 300 μm. From the Fig. 10 it is observed that the transmission curve shifts towards the higher wavelength with the decrease in the length of the fiber, this phenomenon is known as red shift [33] also the transmission spectral curve shifts towards the lower wavelength as the length of the fiber decreases, this occurrence is known as blue shift [34]. The obtained wavelength sensitivity for WBC and RBC with respect to the water is given in Table 2.

Table 3 provides a detailed comparison table highlighting key results between the proposed PCF and previous studies. The table below demonstrates that the proposed sensor outperforms those reported in earlier research.

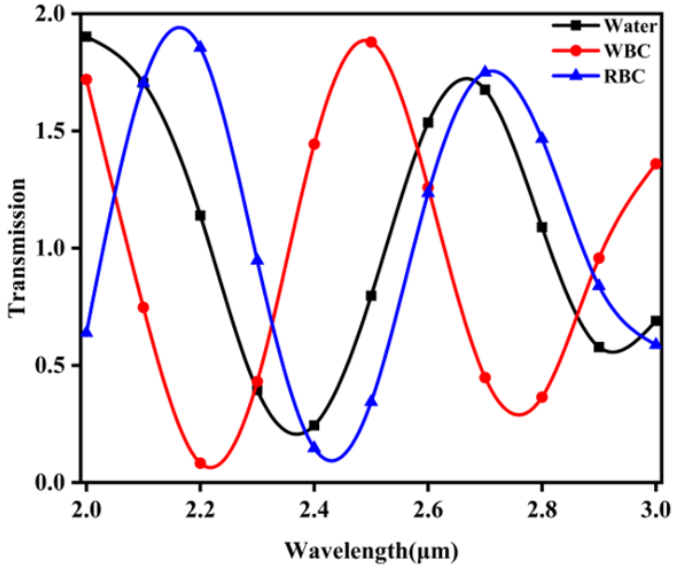

Fig. 10. Transmission spectrum of different blood components.

Table-2. Wavelength sensitivity of the proposed TC-PCF sensor.

Blood Components	Refractive index (n_a)	Wavelength Sensitivity (S_λ) (nm/RIU)
WBC	1.36	1641.2
RBC	1.4	2732.638

Table 3. Examining the suggested PCF in contrast to those previously reported.

Structure and method of sensor	Range of sensing	Wavelength sensitivity (nm/RIU)	Ref.
D-shaped RI PCF sensor	1.33-1.354	294.11	[35]
AZO-coated based PCF-SPR sensor	1.33-1.40	1950	[36]
Au-coated PCF-SPR sensor	1.33-1.36	2200	[37]
Rectangular air-holes in 2 rings	1.33-1.40	2732.638	Proposed work

4. CONCLUSION

A proposed twin-core photonic crystal fiber sensor model aims to detect blood components. Blood sample is to be introduced into this analyte channel for detection. The highest wavelength sensitivity achieved for the proposed sensor is 2732.638 for red blood cell. This sensor offers numerous benefits such as cost-effectiveness, manufacturing tolerance, and straightforward fabrication. Overall, the interplay of mode field distribution, effective refractive index, birefringence, coupling length, and fabrication precision can explain the varying wavelength sensitivity in TC-PCF sensors employing silica as the base material. The results of the proposed TC-PCF are notably superior, rendering and well-suited for detecting blood components.

CONFLICT OF INTEREST

The authors declare that there is no conflict of interests.

REFERENCES

[1] Pinto, A.M. and Lopez-Amo, M., **2012**. Photonic crystal fibers for sensing applications. *Journal of Sensors*, *2012*(1), p.598178.

[2] Bing, P., Huang, S., Sui, J., Wang, H. and Wang, Z., **2018.** Analysis and improvement of a dual-core photonic crystal fiber sensor. *Sensors*, *18*(7), p.2051.

[3] Ehyaee, A., Mohammadi, M., Seifouri, M. and Olyaee, S., **2023.** Design and numerical investigation of a dual-core photonic crystal fiber refractive index sensor for cancer cells detection. *The European Physical Journal Plus*, *138*(2), p.129.

[4] Arman, H. and Olyaee, S., **2021.** Realization of low confinement loss acetylene gas sensor by using hollow-core photonic bandgap fiber. *Optical and Quantum Electronics*, *53*(6), p.328.

[5] Shafkat, A., Rashed, A.N.Z., El-Hageen, H.M. and Alatwi, A.M., **2021.** Design and analysis of a single elliptical channel photonic crystal fiber sensor for potential malaria detection. *Journal of Sol-gel Science and Technology*, *98*, pp.202-211.

[6] Yadav, S., Lohia, P. and Dwivedi, D.K., **2024.** Eminently sensitive mono-rectangular photonic crystal fiber-based sensor for cancer cell detection in THz regime. *Journal of Optics*, *53*(1), pp.528-537.

[7] Chaudhary, V.S., Kumar, D., Mishra, G.P., Sharma, S. and Kumar, S., **2022.** Plasmonic biosensor with gold and titanium dioxide immobilized on photonic crystal fiber for blood composition detection. *IEEE Sensors Journal*, *22*(9), pp.8474-8481.

[8] Hossain, M.B. and Podder, E., **2019.** Design and investigation of PCF-based blood components sensor in terahertz regime. *Applied Physics A*, *125*(12), p.861.

[9] MacPherson, W.N., Gander, M.J., McBride, R., Jones, J.D.C., Blanchard, P.M., Burnett, J.G., Greenaway, A.H., Mangan, B., Birks, T.A., Knight, J.C. and Russell, P.S.J., **2001.** Remotely addressed optical fibre curvature sensor using multicore photonic crystal fibre. *Optics Communications*, *193*(1-6), pp.97-104.

[10] Markin, A.V., Markina, N.E. and Goryacheva, I.Y., **2017.** Raman spectroscopy based analysis inside photonic-crystal fibers. *TrAC Trends in Analytical Chemistry*, *88*, pp.185-197.

[11] Jibon, R.H., Khodaei, A., Priya, P.P., Rashed, A.N.Z., Ahammad, S.H. and Hossain, M.A., **2023.** ZEONEX based hollow rectangular core photonic crystal fiber (PCF) sensor design and numerical investigation for alcohol detection of variant classes. *Optical and*

Quantum Electronics, *55*(11), p.977.

[12] Kaur, V. and Singh, S., **2017.** Extremely sensitive multiple sensing ring PCF sensor for lower indexed chemical detection. *Sensing and bio-sensing research*, *15*, pp.12-16.

[13] Sharma, S., Chaudhary, V.S. and Kumar, D., **2020.** Design of chemical sensor based on dual core photonic crystal fiber. *Materials today: proceedings*, *33*, pp.2122-2124.

[14] Rahaman, M.E., Jibon, R.H., Mondal, H.S., Hossain, M.B., Bulbul, A.A.M. and Saha, R., **2021.** Design and optimization of a PCF-based chemical sensor in THz regime. *Sensing and Bio-Sensing Research*, *32*, p.100422.

[15] Mohamed Nizar, S., Caroline, E. and Krishnan, P., **2021.** Design and investigation of a high-sensitivity PCF sensor for the detection of sulfur dioxide. *Plasmonics*, *16*(6), pp.2155-2165.

[16] Chaudhary, V.S., Kumar, D., Mishra, R. and Sharma, S., **2020.** Hybrid dual core photonic crystal fiber as hydrostatic pressure sensor. *Optik*, *210*, p.164497.

[17] Chen, L., Tian, J., Wu, Q., Li, J., Yao, Y. and Wang, J., **2023.** Temperature-insensitive gas pressure sensor based on photonic crystal fiber interferometer. *IEEE Sensors Journal*, *23*(14), pp.15637-15643.

[18] Liu, Q., Li, S.G. and Chen, H., **2018.** Enhanced sensitivity of temperature sensor by a PCF with a defect core based on Sagnac interferometer. *Sensors and Actuators B: Chemical*, *254*, pp.636-641.

[19] Sharma, P. and Sharan, P., **2015.** Design of photonic crystal based ring resonator for detection of different blood constituents. *Optics communications*, *348*, pp.19-23.

[20] Singh, S. and Kaur, V., **2017, J**uly. Photonic crystal fiber sensor based on sensing ring for different blood components: design and analysis. In *2017 Ninth International Conference on Ubiquitous and Future Networks (ICUFN)* (pp. 399-403). IEEE.

[21] Ahmed, K., Ahmed, F., Roy, S., Paul, B.K., Aktar, M.N., Vigneswaran, D. and Islam, M.S., **2019.** Refractive index-based blood components sensing in terahertz spectrum. *IEEE Sensors Journal*, *19*(9), pp.3368-3375.

[22] Islam, M.R., Iftekher, A.N.M., Mou, F.A., Rahman, M.M. and Bhuiyan, M.I.H., **2021.** Design of a Topas-based ultrahigh-sensitive PCF biosensor for blood component detection. *Applied Physics A*, *127*, pp.1-16.

[23] Eid, M.M., Habib, M.A., Anower, M.S. and Rashed, A.N.Z., **2021.** Hollow core photonic crystal fiber (PCF)–Based optical sensor for blood component detection in terahertz spectrum. *Brazilian Journal of Physics*, *51*, pp.1017-1025.

[24] Bulbul, A.A.M., Jibon, R.H., Biswas, S., Pasha, S.T. and Sayeed, M.A., **2021.** Photonic crystal fiber-based blood components detection in THz regime: Design and simulation. *Sensors International*, *2*, p.100081.

[25] Srivastava, D., Yadav, S., Mishra, A.C., Singh, S., Kumar, V., Lohia, P. and Dwivedi, D.K., **2023.** Ultrasensitive photonic crystal fiber sensor for identifying various explosives. *Plasmonics*, *18*(6), pp.2295-2304.

[26] Yadav, S., Singh, S., Lohia, P., Umar, A. and Dwivedi, D.K., 2**022.** Delineation of profoundly birefringent nonlinear photonic crystal fiber in terahertz frequency regime. *Journal of Optical Communications*, (0).

[27] Chaudhary, V. and Singh, S., **2023.** Highly sensitive twin core photonic crystal fiber for hazardous cancer cell detection in THz frequency regime. *Optical and Quantum Electronics*, *55*(13), p.1174.

[28] Mollah, M.A., Yousufali, M., Ankan, I.M., Rahman, M.M., Sarker, H. and Chakrabarti, K., **2020.** Twin core photonic crystal fiber refractive index sensor for early detection of blood cancer. *Sensing and Bio-Sensing Research*, *29*, p.100344.

[29] Huang, W.P., **1994.** Coupled-mode theory for optical waveguides: an overview. Journal of the Optical Society of America A, *11*(3), pp.963-983.

[30] Srivastava, D., Yadav, S., Mishra, A.C., Singh, S., Lohia, P. and Dwivedi, D.K., **2024.** Numerical study of photonic crystal fiber-based optical biosensor for detection of cervical cancer. *Journal of Optics*, *53*(2), pp.1155-1162.

[31] Hossain, M.B., Islam, S.R., Hossain, K.T., Abdulrazak, L.F., Sakib, M.N. and Amiri, I.S., **2020.** High sensitivity hollow core circular shaped PCF surface plasmonic biosensor employing silver coat: A numerical design and analysis with external sensing approach. *Results in Physics*, *16*, p.102909.

[32] Panda, A. and Pukhrambam, P.D., **2021.** Investigation of defect based 1D photonic crystal structure for real-time detection of waterborne bacteria. *Physica B: Condensed Matter*, *607*, p.412854.

[33] Liu, W., Wang, F., Liu, C., Yang, L., Liu, Q., Su, W., Lv, J., An, S., Li, X., Sun, T. and Chu, P.K., **2020.** A hollow dual-core PCF-SPR sensor with gold layers on the inner and outer surfaces of the thin cladding. *Results in Optics*, *1*, p.100004.

[34] Portosi, V., Laneve, D., Falconi, M.C. and Prudenzano, F., **2019.** Advances on photonic crystal fiber sensors and

applications. *Sensors*, *19*(8), p.1892.

[35] Azab, M.Y., Hameed, M.F.O., Mahdiraji, G.A., Adikan, F.R.M. and Obayya, S.S.A., **2022.** Experimental and numerical characterization of a D-shaped PCF refractive index sensor. *Optical and Quantum Electronics*, *54*(12), p.846.

[36] Islam, M.R., Iftekher, A.N.M., Noor, F., Khan, M.R.H., Reza, M.T. and Nishat, M.M., **2022.** AZO-coated plasmonic PCF nanosensor for blood constituent detection in near-infrared and visible spectrum. *Applied Physics A*, *128*(1), p.86.

[37] Hasan, M.R., Akter, S., Rifat, A.A., Rana, S. and Ali, S., **2017,** March. A highly sensitive gold-coated photonic crystal fiber biosensor based on surface plasmon resonance. *Photonics.* 4(1), p. 18**.**

